科学通报 2019 年 第 64 卷 第 22 期: 2305 ~ 2315
评 述
《中国科学》杂志社
SCIENCE CHINA PRESS

岩石圈中部不连续面的成因及其动力学意义

徐义贤[1*], 郑建平[2], 杨晓志[3], 夏群科[1]

1. 浙江大学地球科学学院, 杭州 310027;
2. 中国地质大学地球科学学院, 武汉 430074;
3. 南京大学地球科学与工程学院, 南京 210023

* 联系人, E-mail: xyxian@zju.edu.cn

2019-03-04 收稿, 2019-06-10 修回, 2019-06-12 接受, 2019-07-15 网络版发表
国家自然科学基金(41530319, 41830212)资助

摘要 地球物理和岩石地球化学研究揭示岩石圈地幔在物性和化学组成上极为不均一, 保存了地球演化的大量记录. 近20年来的地震学探测结果, 指示大陆岩石圈中部广泛存在速度不连续面, 大多表现为速度明显降低的梯度带, 与各向异性和地幔浅部的高导层有较好的一致性, 主要分布在60~120 km深度. 但是, 其成因目前尚未形成共识. 在经典板块构造的框架内, 基于已有的对岩石圈和岩石圈-软流圈边界的认识, 我们追溯了岩石圈中部不连续面的地球物理探测历程及其主要结果, 给出了地震学定义的岩石圈中部不连续面的矿物岩石学解释和大地电磁资料提供的电性约束信息. 在梳理目前的主要解释模型后, 重点介绍了岩石圈中部不连续面是"冻结的"大洋岩石圈-软流圈边界的观点, 并进一步拓展为一种工作模型—动态演化的LAB模型, 依此讨论了这一解释模型潜在的重要动力学意义. 我们认为, 对岩石圈中部不连续面开展多学科的综合研究, 有可能为突破经典板块构造假说提供新的机会, 中亚显生宙增生型岩石圈和华北板块岩石圈是研究这一问题极好的天然实验室.

关键词 岩石圈中部不连续面, 负速度梯度带, 高导层, 各向异性, 含水矿物, 板块构造

岩石圈是指地球表层黏度大的外壳, 可以在地质演化历史上长时间支撑差异应力; 岩石圈之下为黏度较小的软流圈, 软流圈内允许与均衡调整相关的物质流动[1]. 岩石圈与软流圈的边界(lithosphere-asthenosphere boundary, LAB)是经典板块构造学说中的必备元素. 不同学科对岩石圈和软流圈的定义有所不同, 根据热传导机制, 岩石圈被认为对应于上地幔热边界层以上的部分, 即岩石圈内的热传输为纯传导机制, 其下伏软流圈顶面位于地幔岩固相线附近, 软流圈内部热传输可能是对流和传导两种方式并存, 但以对流机制为主, 因此LAB是温度控制的界面[2]. 由于大陆岩石圈的厚度变化范围很大, 如某些显生宙岩石圈地幔厚度不足100 km, 而前寒武克拉通型岩石圈的厚度可以超过300 km, 因此岩石地球化学家对LAB有不同的理解[3]. 对于大洋岩石圈, 一个最具代表性的观点认为LAB是地球化学组分边界: 软流圈由含水且化学上饱满的(fertile)橄榄岩如二辉橄榄岩组成, 而岩石圈地幔主要由亏损的辉橄岩组成, 它是干的且化学上贫瘠的(sterile)橄榄岩[4]. 对于大陆克拉通, 亏损岩石圈地幔一般可以深达200 km以上, 以产生足够的浮力补偿相对较低的温度[5~7], 并保证岩石圈地幔可以与其上覆地壳紧密连成一体长达数十亿年[8,9]. 这一模型与Jordan提出的大陆构造圈模型基本一致, 此时LAB是化学和热的总浮力处处相等的面[1,5].

地震学家Gutenberg[10,11]最先发现上地幔低速层, 随后, Lehmann[12~14]发现上地幔约220 km存在一波速

引用格式: 徐义贤, 郑建平, 杨晓志, 等. 岩石圈中部不连续面的成因及其动力学意义. 科学通报, 2019, 64: 2305–2315
Xu Y X, Zheng J P, Yang X Z, et al. The origins and geodynamic implications of mid-lithospheric discontinuities (in Chinese). Chin Sci Bull, 2019, 64: 2305–2315, doi: 10.1360/N972019-00161

© 2019《中国科学》杂志社

向下增加的界面. 为纪念上述发现, 上地幔低速层的顶面和底面分别命名为G不连续面和L不连续面. 历史上, 不同的研究者曾将LAB归结为G不连续面和/或L不连续面. 在PREM(preliminary reference Earth model)模型中, L不连续面作为上地幔内220 km左右低速带的下界[15]. 综合几十年来的研究成果, 大多数指示软流圈为上地幔部分熔融带, 其熔融程度和熔体赋存形式仍存在争论, 但足以使我们认定G不连续面与LAB相当, 而L不连续面与软流圈底界面相当.

随着深部探测技术的发展, 根据测定方法的不同, 岩石圈厚度具有不同的定义[16]. 探测岩石圈的地震学方法可以分为三类: 速度层析成像、界面成像、各向异性检测. 第一类方法获得岩石圈速度结构后, 可以用上地幔低速层的顶面深度或最大负梯度对应的深度作为岩石圈的厚度. 在第二类方法中, Ps接收函数受壳内多次波的干扰严重, 仅适用于上地幔浅部界面(一般<100 km)成像, 因而利用Sp接收函数是上地幔速度界面成像的主要方法. 在Sp接收函数图像上, 大陆上地幔一般出现1个或多个横向连续或断续可追踪的负速度梯度带. 有必要指出, 由于大陆LAB多数显示为速度变化较小的负梯度带, 因此利用Sp接收函数对大陆LAB的成像分辨率并不高(Sp震相常用频率对应的波长大约在16~160 km之间). 第三类方法中, 远震S波分裂检测给出的是整个上地幔各向异性叠加的结果; 面波径向各向异性的检测结果较为稳定, 但深度分辨率较低; 体波和面波走时反演或波形拟合给出的各向异性参数稳定性较差. 关于上地幔径向和方位各向异性的地震检测方法, Selway等人[17]做了较为系统的总结. 一般认为岩石圈地幔的各向异性主要反映岩石圈形成和/或后继构造热事件中保留下来的变形特征, 属于继承性各向异性, 而软流圈各向异性主要反映现今的软流圈物质流动方向, 因而可以根据检测到的上地幔各向异性结构的变化来确定岩石圈厚度[18,19]. 在全球平均意义上, LAB的地震学观测值大于根据岩石捕虏体确定的化学边界层深度, 而与热边界层定义的岩石圈厚度较为一致[20].

大地电磁学是另一种确定岩石圈厚度的有效方法. 大陆岩石圈地幔的电阻率一般在50~200 Ωm, 远低于中上地壳(>1000 Ωm), 但与下地壳的电阻率接近; 软流圈地幔的电阻率典型值在5~25 Ωm之间[21]. 由于软流圈地幔和岩石圈地幔的电阻率相差几倍到几十倍, 因此大地电磁测深结果对确定岩石圈厚度具有重要意义. 但需要指出的是, 壳内低阻层如某些地区发育的低阻下地壳, 可能成为探测上地幔低阻层的“屏障”. 全球统计结果表明[22], 大地表面热流和上地幔低阻层的埋深具有很高的相关性, 揭示根据上地幔低阻层顶面确定的LAB和热边界层深度较为一致[16,18], 可以与地震学结果相互印证.

由于岩石圈的厚度与其形成后的岩浆作用、交代作用和变质作用相关, 因而可能是一种动态的界面[3]. 有趣的是, 我们几十年来探测LAB的努力, 虽没有达成对LAB的精确定义和其成因上的共识, 但却为认识岩石圈的内部结构及其时空演化积累了大量实证资料. 一个突出的例子, 就是发现了大陆岩石圈地幔不仅横向上极为不均一, 而且在纵向上存在岩石圈中部不连续面(mid-lithospheric discontinuities, MLDs), 这是经典的一维地震学模型如PREM模型所缺失的特征. 本文试图对近年来不断报道的MLDs的属性和成因及其动力学意义进行评述.

1 从LAB到MLD

自20世纪70年代始, 地球物理学家利用深反射地震技术, 陆续探测到莫霍面下方仍有明显的反射面[23~29], 这些地幔反射面大多位于大陆古缝合带或造山带下方, 因而一般解释为残留、继承或“冻结的(frozen in)”俯冲带结构[27,30], 亦或理解为与造山作用相关的岩石圈地幔剪切带[31,32]. 两个例外但很有意义的解释来自Thybo和Perchuć[26]与Yang[28], 前者从全球大陆超长反射地震剖面上识别出所谓的8°(广角反射波大约在炮检距8°左右出现)地幔低速带, 并认为其成因受温度控制因而最可能是部分熔融造成; 后者从东大别造山带短反射地震记录上, 识别出莫霍面下方50~80 km深度存在多层地幔反射面, 并将其与扬子克拉通和华北克拉通的碰撞造山、及中国东部晚中生代发生的岩石圈减薄事件相联系, 因而认为岩性即化学组分的不同是形成这些地幔反射面的成因. 上地幔地震不连续面的这两种解释, 对于认识后述岩石圈中部地震不连续面的成因具有重要意义.

在全球范围内, 采用Ps或Sp震相的接收函数成像、面波层析成像及SS前驱波成像技术, 近年来不断探测到大陆岩石圈地幔内部存在地震不连续面或速度梯度带, 其深度范围主要集中在60~120 km(图1), 绝大多数指示为速度负梯度带, 速度降低大多在3%~9%范围, 某些区域可达10%以上, 并在其内部或上下相邻深

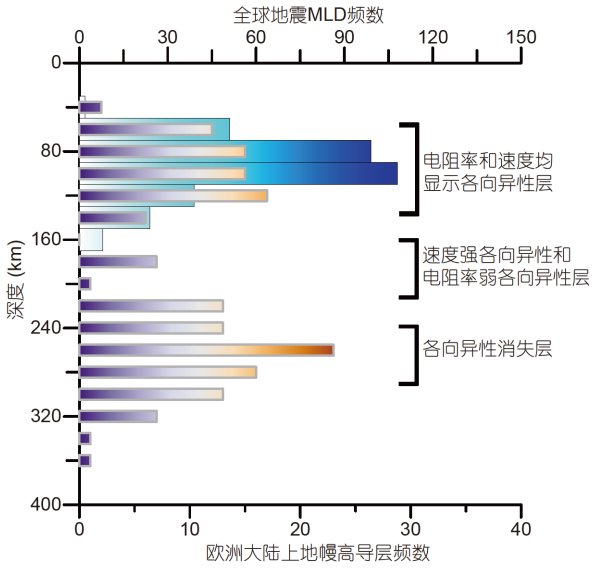


图 1 (网络版彩色)全球探测到的地震MLD和欧洲大陆上地幔高导层(MHCL)随深度的频数分布. 地震MLD数据综合自文献[17,33~35]. 欧洲上地幔高导层深度分布取自文献[36]. 注意上地幔高导层深度的第一个峰值60~120 km对应欧洲大陆显生宙岩石圈, 而第二个峰值220~320主要对应欧洲大陆的早前寒武纪岩石圈. 高导层第一个峰值区间存在明显的速度各向异性, 暗示其成因与组分的定向分布和/或构造因素如剪切相关; 高导层第二个峰值区间无明显地震各向异性, 可以用广泛的部分熔融层来解释

Figure 1 (Color online) The frequency distribution of global seismic mid-lithospheric discontinuities (MLDs) and the upper mantle high electrical conductivity layers (MHCLs) in continental Europe. Seismic MLDs are synthesized from [17,33–35]. The MHCLs in Europe is taken from Ref. [36]. The first peak of MHCLs in depths of 60–120 km corresponds to the Phanerozoic lithosphere, while the second peak of MHCLs in depths of 220–320 km corresponds mainly to the Early Precambrian lithosphere. Velocity anisotropy presents generally corresponding to the first peak interval of MHCLs, suggesting that the origin of MLDs may be related to the directional distribution of compositions and/or structural factors such as shear. No obvious seismic anisotropy presents in the second peak interval of MHCLs, which can be ascribed to a extensive partial melting layer

度, 发现了速度方位和/或径向各向异性特征[19,37~49]. 主要探测结果已经收录于*Lithospheric Discontinuities*[51]一书中. 由于它们的深度明显小于温度定义的LAB[16], 而与成熟的大洋盆地的LAB相当[52], 因而Fischer等人[18]首次建议称其为岩石圈中部不连续面 (MLDs).

在大洋岩石圈和显生宙大陆岩石圈, MLD与LAB在深度上无法区分或MLD不可见. Tharimena等人[50]利用SS前驱波和长达24年的远震数据, 在太平洋板块年龄小于36 ± 9 Ma的区域, 探测到30~80 km深度广泛发育尖锐的速度不连续面, 在<21 km深度内速度急剧下降了3%~15%, 而且年龄越年轻该界面越浅, 因而可以合理地解释为部分熔融层的顶界; 在年龄大于36 Ma区域, 该界面与年龄无关而稳定在60 ± 1.5 km深度, 作者因而用冻结的熔体层来解释. Hopper和Fischer[53]利用Sp接收函数CCP叠加技术, 发现美国西部构造活动区的上地幔负速度梯度带(negative velocity gradients, NVGs)位于60~90 km, 速度减少幅度达到10%±4.5%, 因而也可以合理地解释为部分熔融层的顶界, 即LAB. Calò等人[33]利用单台高质量长期观测数据, 采用互卷积获得的体波散射震相和面波(Love和Rayleigh)频散数据进行联合反演, 结果指示美国西部构造活动区的LAB位于60~130 km深度, 这与Hopper和Fischer[53]的结果有一定差异. 在美国东部显生宙岩石圈特别是在新英格兰和弗吉尼亚地区, Hopper和Fischer[53]发现上地幔NVGs变化剧烈, 深度位于50~115 km(平均为76±10 km), 速度减少幅度达到6.5% ± 4%, 因而也倾向于用LAB来解释.

克拉通地区探测到的MLDs与LAB深度差异很大, 甚至出现多个岩石圈地幔中部不连续界面[19,33], 而且MLDs内部可能出现复杂的组合结构. Hopper和Fischer[50]发现美国中北部克拉通地区的LAB难以识别, 而以NVGs为特征的MLD位于70~100 km深度, 对应的Sp负相强度与地体年龄有较好相关性, 年龄越老强度越大. Calò等人[33]发现美国中北部克拉通地区的LAB深度大于170 km, 在100~130 km(剪切波速度由高变低)和150~170 km(剪切波速度由低变高)深度分别出现MLD, 表征上地幔剪切波低速带的顶底界面; 时代越老的地区岩石圈地幔的成层性越好, 相应的MLDs界面处速度变化越显著. Kind等人[55]利用Sp接收函数发现欧洲显生宙地区(如潘农盆地)的LAB位于70~80 km 深度, 而向东进入东欧克拉通之后, 转换为100 km左右的MLD, 因此作者们认为这一结果给出了克拉通活动边缘的LAB转换为克拉通内部MLD的实证. Sun等人[54]综合P波反射系数、径向各向异性及电阻率数据, 研究了西澳大利亚克拉通的MLDs精细结构, 发现在西澳克拉通下方存在2条连续的有一定厚度的MLDs, MLDs内部表现为叠层结构(高低速交替的层状结构), 而不是速度单调增加或降低.

地震学研究还表明克拉通地区的MLDs可能与各向异性相关[17,19,43,49,56]. Yuan和Romanowicz[43]与Yuan等人[56]基于北美克拉通地区方位各向异性随深度变化及其与各向同性NVGs的关系, 认为MLDs可能起因于方位各向异性的突变. Ford等人[19]在北美克拉通地区同样探测到岩石圈中部存在方位各向异性边界, 但是并不精

确对应以各向同性NVGs定义的MLDs. 实际上, 当不出现各向同性NVGs的情况下, 仅由方位各向异性边界产生Sp接收函数的负相, 仍存在技术上的不确定性[17].

值得提及的是, 大范围的人工源广角反射/折射剖面[57,58]及接收函数研究[59,60]均揭示, 岩石圈地幔内部也存在速度陡增界面, 表征速度达到8.4~8.5 km/s的顶面[57], 可以归结为Hales不连续面[61], 一般解释为存在各向异性层[62]或岩石圈地幔内部有随机分布的具有较大长宽比的不均匀散射体[63]. 实际上, Calò等人[33]在美国中北部克拉通地区150~170 km深度检测到的剪切波速度由低变高的MLD也可视为Hales不连续面.

MLD所在深度除了相对较低的波速外, 往往还具有较低的电阻率[64], 如在欧洲大陆显生宙岩石圈地区(图1, 文献[36]), 电阻率范围一般为10~100 Ωm. 我们最新的研究结果表明, 美国中北部克拉通地区的MLD还与低阻各向异性层对应: 在未发生垮塌的Trans-Hudson造山带南部[65], 低阻各向异性层位于约70 km深度, 而在与其相邻的发生过显生宙强烈底侵作用的Superior克拉通南部, 低阻各向异性层则位于约100 km深度, 它们的最小电阻率可以低至1~10 Ωm(图2). 这个例子至少说明在北美克拉通地区MLDs的低速、低阻及各向异性在空间上相关, 从而要求解释MLDs的成因模型

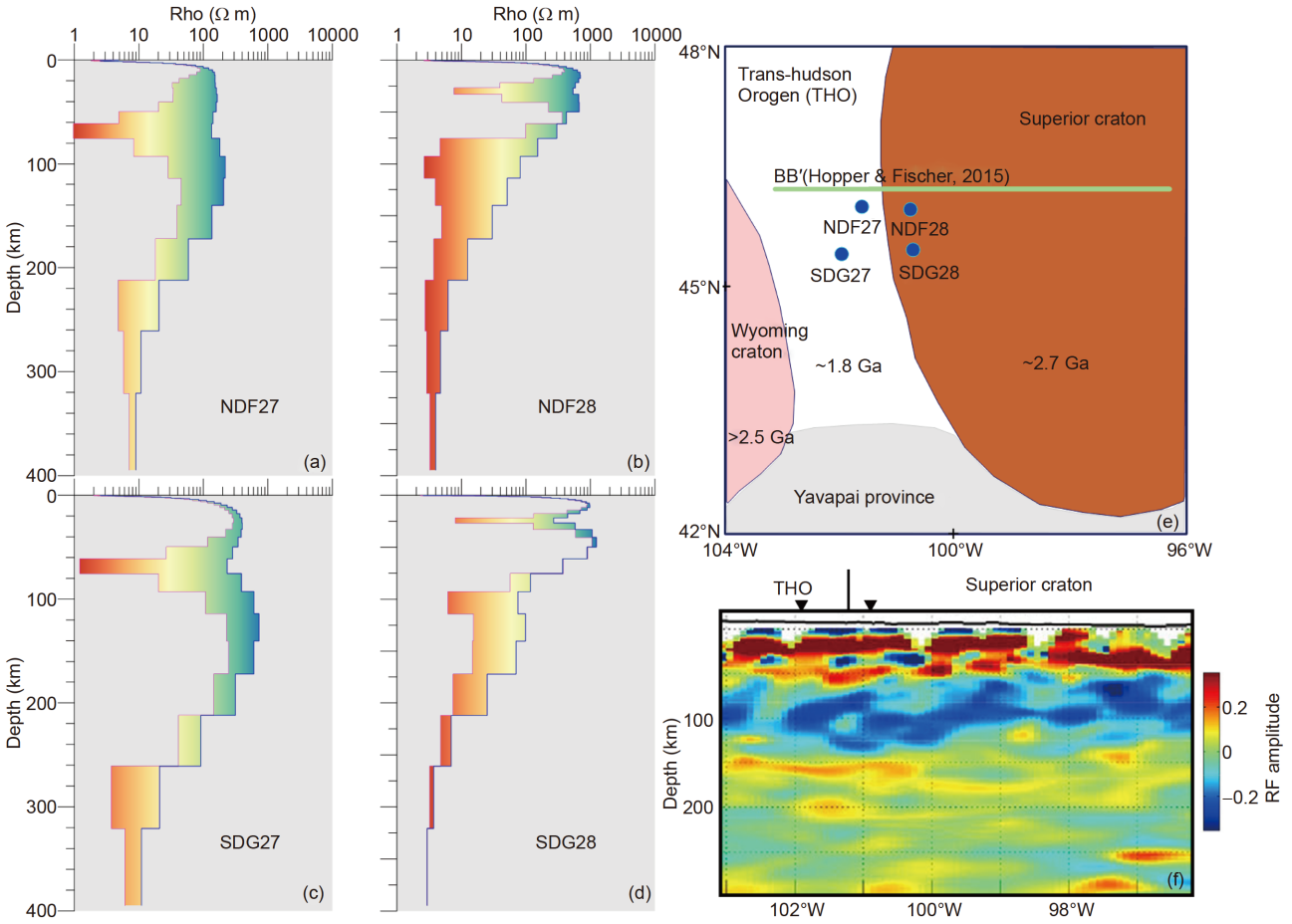


图 2 美国北部Trans-Hudson造山带(e中测点NDF27和SDG27)和Superior克拉通(e中测点NDF28和SDG28)内大地电磁资料一维各向异性反演的结果(a)~(d)及其与远震Sp转换震相接收函数成像结果(f)的比较. (a)~(d)中红色折线为最小电阻率曲线, 蓝色折线为最大电阻率曲线, 它们之间的差异(填充颜色区域的宽度)代表方位各向异性的强度. (e) 为大地构造简图. (f) 取自文献[66]中BB′测线, 大地电磁测点SDF27和SDF28以倒三角分别标注在剖面的Trans-Hudson造山带和Superior克拉通

Figure 2 The results of 1-D anisotropic inversion (a)–(d) of magnetotelluric data in Trans-Hudson Orogen (THO) (NDF27 and SDG27) and Superior Craton (NDF28 and SDG28) in the northern United States, which are compared with the results of teleseismic receiver functions of Sp-converted phases (f). The red and blue lines present the minimum and maximum resistivities through (a)–(d), respectively. The difference between the minimum and maximum resistivities represents the strength of azimuthal anisotropy. (e) A tectonic sketch of the middle northern U.S. (f) From the BB′ line of Ref. [66] and marked in (e), MT stations SDF27 and SDF28 are labeled as Trans-Hudson Orogen and Superior craton in inverted triangle, respectively

必须可以同时解释其地震学结构和电性结构.

综上，从现有的地震学和大地电磁学探测结果来看，克拉通内部的MLDs多数对应各向同性的NVGs，不论是分布的深度范围还是其内部的结构都是相当复杂的，还需要发展更高分辨的探测方法技术和开展更多的实际探测.

2 MLDs的地震学和电学性质的矿物岩石学解释

在不考虑变形、各向异性和黏弹性等效应的情况下，岩石的地震波速主要取决于其矿物成分和熔/流体含量. 含挥发分地幔橄榄岩的固相线温度，在60~70 km深度时为1000°C左右[67,68]. 挥发分强烈影响着熔/流体在岩石圈地幔中的行为，一方面CO_2和H_2O可能诱发深部地幔岩石的部分熔融而产生熔体，另一方面含碳酸盐的熔/流体在上升过程中会穿越固相线发生固结，因此岩石圈地幔内部可能存在含熔/流体的低速低阻层. 由于熔体较固态岩石矿物组合具有更好的导电性，许多学者往往将浅部地幔的高导异常归因于熔体. 定量研究发现，要拟合大地电磁观测到的低阻异常电阻率，需要的玄武质熔体的含量大约为1%~10%，且要求体系的温度达到1400°C左右[69~71]，这对于多数地区的浅部地幔来说不现实[72]. 基于此，一些学者提出了碳酸盐熔体可能是形成浅部地幔低阻异常的重要机制[73,74]：同等条件下，碳酸盐熔体的电阻率比玄武质熔体低几个数量级，只需要约0.1%的碳酸盐熔体就可以产生10~100 Ωm的电阻率，且体系的温度只需要1000°C左右. 然而，碳酸盐熔体在浅部地幔中是不稳定的[72]. 另外，有学者认为即使少量碳酸盐熔体能够在浅部地幔稳定存在，这些熔体的赋存主要由表面张力控制，难以形成熔体的定向排列和电导率的各向异性[75]. 因此，对于克拉通岩石圈地幔来说，大部分已知MLDs对应的温度低于含挥发分地幔橄榄岩的固相线[76]，MLDs的低速、低阻及各向异性特征难以用熔体来解释.

含水矿物如角闪石和金云母，具有比橄榄石、辉石、石榴子石和尖晶石等名义上无水矿物更低的地震波速[77]，因此交代作用形成的角闪石和金云母等典型含水矿物，可以有效降低地幔岩的地震波速[34,78]. 一些学者根据模拟计算提出地幔含水矿物可以解释世界上典型克拉通岩石圈地幔中的地震低速带[17,79]. 巧合的是，前人的岩石学研究也证实，古老克拉通岩石圈地幔在~100 km深处存在一个富集含水矿物的交代层[6,80]. 地幔捕虏体的温压研究表明，含角闪石的地幔岩多产于100 km以浅[17]，含金云母的地幔捕虏体更为普遍且其稳定深度可达150 km以上. 可见，它们的稳定深度在MLDs埋深的变化范围之内(图3). 新的实验研究表明：如果有10%含水和二氧化碳的熔体，在克拉通地区MLDs深度对应的温压条件下结晶，将可以分别产生9.5 wt%的角闪石和6 wt%的金云母[81]，相应地可以引起剪切波速度降低达到6%的水平[53,81]，符合大多数全

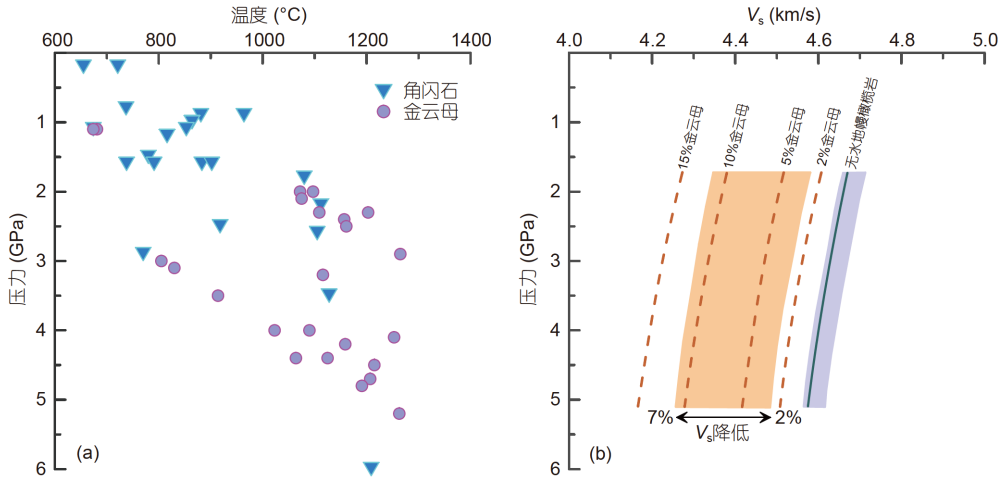


图 3 (网络版彩色)上地幔主要含水矿物的稳定温压范围及其对剪切波速度的影响. (a) 含金云母、角闪石地幔捕虏体的深度(修改自文献[34]); (b) 金云母含量降低地幔橄榄岩的地震波速的相图(修改自文献[78])

Figure 3 (Color online) Temperature and pressure range of major water-bearing minerals in upper mantle and its effect on shear-wave velocity. (a) The pressure and temperature ranges for phlogopite and amphibole from mantle xenoliths (modified from Ref. [34]; (b) relationships of phlogopite content versus seismic velocity decrease of mantle peridotite (modified from Ref. [78])

球MLDs的地震学观测(2%~7%)[34], 这一研究结果无疑为含水相矿物在岩石圈地幔形成富集层即MLDs提供了新的证据. 另一方面, 由于岩石圈地幔内部的挥发分主要和含水相矿物共生, 近年来的高温高压实验发现: 含挥发分的含水相矿物一般都具有较低的电阻率, 同等条件下可以比橄榄岩低几个数量级[82,83], 只要它们在浅部地幔少量出现(比如百分之几的体积含量, 主要取决于环境温度和传导相矿物的连通性), 就可以显著降低全岩体积电阻率, 并与大地电磁观测结果相当[82~86]. 因此, 我们有理由相信克拉通岩石圈内部的熔体/流体交代作用和/或熔体结晶作用, 对MLDs的形成起到了重要作用.

3 MLDs的成因及其动力学意义

随着MLD的不断发现, 其成因引起了固体地球科学家们的极大兴趣[17,20,34,76,78,87,88]. 根据MLD的地震学特征和随地质时代的演化规律, 目前已提出包括化学组分变化[17]、弹性调整的颗粒边界滑动[20](elastically accommodated grain-boundary sliding, EAGBS)、上地幔分层各向异性[43], 以及"冻结的"LAB[34]等解释模型, 其中"冻结的"LAB模型引人关注.

此处将"冻结的"LAB模型拓展为一种工作模型—动态演化的LAB模型: MLD开始于大洋岩石圈的LAB, 其深度从洋中脊到俯冲带因受控于温度(因而年龄)而逐渐增大; 在大陆增生过程中, 大洋岩石圈的LAB通过后述几种可能的机制"遗传"给大陆岩石圈, 然后随大陆岩石圈冷却, LAB向深部迁移, 老的LAB"冻结"在大陆岩石圈内部而形成MLD[34]. 大洋岩石圈的LAB"遗传"给大陆岩石圈, 并成为大陆MLD的可能机制至少可以包括: (1) 活动板块边界"夭折的"洋陆俯冲或洋内俯冲, 如美国怀俄明克拉通[64]和西准噶尔显生宙岩石圈[89,90]; (2) 通过多陆块围限而最终"捕获"的大洋板块成为大陆的一部分, 如地中海东部[91]和显生宙增生区的塔城盆地的基底[92]; (3) 通过被动板块边界的横向拼贴, 如现今大西洋两侧; (4) 直接继承自板块构造起始之前已逐渐冷却的岩浆洋外壳. MLD形成后, 由于其特定的深度和相应的温压条件, 在后期岩浆作用、变质作用及构造运动的叠加改造过程中, 可能成为岩石圈地幔内含水相矿物和挥发分进一步富集的区域, 在区域尺度上可以表现为地幔岩浆交代作用的"前锋带"[6], 也可以演变为板块运动的拆离带[93,94], 造成其结构已远比大洋岩石圈的LAB复杂得多. 这一模型不仅可以成功解释目前探测到的MLDs的各种地球物理性质, 而且可以融合各种假设, 如MLDs作为岩石变形机制转变的界面[20,95]、或矿物颗粒粒径由细颗粒转变为粗颗粒的界面[96].

假设非洲大陆岩石圈由MLD与其下伏岩石圈根解耦, 利用地球动力学模拟技术, Wang等人[93]重建了大约自130 Ma以来, 非洲大陆MLD以上部分的岩石圈向东北方向运动, 并覆于印度洋岩石圈之上, 留下的岩石圈根圈闭于大西洋岩石圈, 从而提供了解释大陆板内出现大洋型玄武岩而大洋可以捕获大陆岩石圈的一种新机制. 根据Wang等人[93]的模拟研究, 若MLD的有效黏度为10^{19}~5×10^{20} Pa s且MLD的厚度在10~50 km之间时, 非洲大陆上下岩石圈的解耦速率可以达到0.5~1.5 cm/a, 其中MLD的有效黏度越低或者其厚度越大, 解耦速率越大. 因此, 根据该研究我们认为, 当MLD的有效黏度比其上下大陆岩石圈的有效黏度(一般在10^{21}~5×10^{24} Pa s之间)[17]低一个量级左右及以上时, 具有一定厚度(>10 km)的MLD可以产生上下岩石圈的解耦. 上述机制若成立, 无疑说明在某些情况下, 如被动型板块边界带, 当软流圈相对"干"或岩石圈底部阻力相对强的情况下, MLD对板块构造的动力学意义和 LAB相同[93].

鉴于MLD在全球广泛分布, 具有深度较浅, 且低速低阻因而黏度低, 以及各向异性等特征, 我们进一步推测: 如图4所示, LAB是主要由温度控制的、随岩石圈年龄逐渐变深的部分熔融带, 而MLD实际上构成了板块运动的滑动带. 对年青岩石圈, 由于地温梯度大, LAB较浅, 并由于减压效应下伏软流圈的熔体分数较高, 因而LAB与MLD不可分; 对古老岩石圈, 由于地温梯度小, LAB较深, 下伏软流圈的熔体分数低(相对"干"的软流圈), 此时MLD与LAB在深度上可以较好区分, MLD遂成为上覆板块的滑动带. 这一假说的优势至少包括: (1) 板块运动是在较浅的深度上进行的, 板块运动的效率可以更高, 从而易于理解某些板块特别是古老克拉通的快速运动; (2) MLD处的温度可以有高达300°C以上的差异, 因而热力成为板块构造驱动力中的重要控制因素, 从而解决被动大陆边缘难以发育俯冲带的难题[98]; (3) 可以解释大洋盆地为何具有大陆磁异常特征的基底[99], 同时协调洋岛玄武岩(OIB)及洋中脊玄武岩(MORB)在地球化学特征上的差异[100].

4 展望

对MLDs的探测方兴未艾[20,51,81]. 前述MLDs成因解释模型中, 大洋岩石圈的LAB如何"遗传给"大陆岩

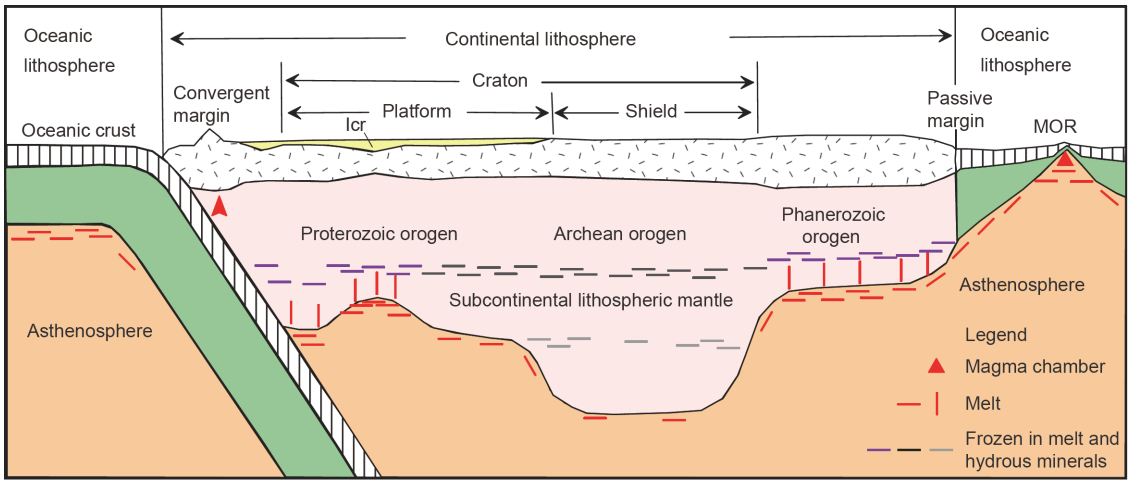


图 4 大陆岩石圈及被动边界和收敛边界断面概念图(修改自文献[97]). 图中假设前寒武纪克拉通岩石圈厚度为200~250 km, 大洋岩石圈大约100 km. icr代表陆内裂谷, MOR表示洋中脊. 红色三角表示岩浆房, 红色短线及密度表示熔体及其富集程度, 淡黑色、黑色及紫色短线分别表示不同时代"冻结的"熔体及其交代作用生成的含水(及含挥发分)矿物

Figure 4 Conceptual cross-section of continental lithosphere with passive and convergent boundaries (revised from Ref. [97]. It is assumed that the Precambrian craton lithosphere is 200−250 km thick and the oceanic lithosphere is about 100 km thick. The icr and MOR stand for the intracontinental rift and the mid-ocean ridge. Red triangle indicates magma chamber, red short line and its number indicate melt and its enrichment degree, and light black, black and purple short line indicate volatile-bearing minerals produced by "frozen" melt and related metasomatism in different ages, respectively

石圈的机制尚不清晰, 它涉及大陆地壳的形成和大洋岩石圈的联系、俯冲板块的命运、以及大洋岩石圈是否可以直接克拉通化等重大科学问题, 解剖增生型岩石圈如中亚地区可以为回答这一问题提供关键证据. 其次, 后期热构造事件改造大陆岩石圈MLDs的机制及其后效也不清晰, 它涉及深部岩浆、变质和交代作用、以及挥发分(包括水)的循环, 美国西部的盆山省和中国华北板块应是解开这一谜底的天然实验室. 开展这一方向的研究具有重要的科学意义, 需要地球物理、岩石学及地球化学学科紧密协作.

在不断更新的全球地震学模型上, 在大陆岩石圈地幔确实可以观测到存在全球性的S波速度低速带[101], 并且与太平洋岩石圈的LAB相当[102], 即可能存在全球意义上的地震MLDs, 暗示它可能与板块构造具有关联性. 板块构造假说虽然已经在教科书中定义为板块构造理论, 但质疑从未间断. 一个流行的质疑是其无法解释大陆构造, 尤其是前寒武大陆构造, 因而引发了对"板块构造何时起始? "的全球性讨论, 并分别于2006年在美国怀俄明州和2016年在瑞士苏黎世召开了两次重要国际会议, 但迄今没有达成广泛的共识. 对比大洋和大陆岩石圈地幔的组成和结构, 追溯大洋岩石圈和大陆岩石圈的协同演化规律, 可以提供地壳部分严重缺失的信息. 本文讨论的MLDs的分布规律、性质及成因解释, 将大陆岩石圈地幔与大洋岩石圈地幔通过地球构造体制及其演化联系了起来, 有可能为突破经典板块构造假说提供新的机会.

致谢 与浙江大学杨文采院士和杨树峰院士及陈汉林教授、中国科学院地质与地球物理研究所陈凌研究员、中国地震局地球物理研究所吴庆举研究员、中国地震局地震预测研究所高原研究员、中国科学技术大学张海江教授、中国科学院南海海洋研究所王志教授、华中科技大学王慧琳副教授, 以及澳大利亚麦考瑞大学的杨英杰副教授、美国圣路易斯大学的朱露培教授等, 进行了广泛而深入的交流, 浙江大学刘书钰提供了图2中的反演结果, 对于他们的贡献, 作者特此致谢! 同时, 感谢审稿人给出的建设性的修改建议.

参考文献

1 Jordan T H. Composition and development of the continental tectosphere. Nature, 1978, 274: 544–548
2 Sleep N H. Evolution of the continental lithosphere. Annu Rev Earth Planet Sci, 2005, 33: 369–393
3 O'Reilly S Y, Griffin W L. The continental lithosphere-asthenosphere boundary: Can we sample it? Lithos, 2010, 120: 1−13
4 Herzberg C. Geodynamic information in peridotite petrology. J Petrol, 2004, 45: 2507–2530

5 Jordan T. Structure and formation of the continental tectosphere. J Petrol, 1988, (1): 11–37
6 Griffin W L, O'Reilly S Y, Afonso J C, et al. The composition and evolution of lithospheric mantle: A re-evaluation and its tectonic implications. J Petrol, 2009, 50: 1185–1204
7 Lee C T A. Geochemical/petrologic constraints on the origin of cratonic mantle. In: Benn K, Mareschal J C, Condie K C, eds. Archean Geodynamics and Environments. Washington DC: AGU Publication, 2006, 164: 89–114
8 Pearson D G, Carlson R W, Shirey S B, et al. Stabilisation of Archaean lithospheric mantle: A ReOs isotope study of peridotite xenoliths from the Kaapvaal craton. Earth Planet Sci Lett, 1995, 134: 341–357
9 Carlson R W, Pearson D G, James D E. Physical, chemical, and chronological characteristics of continental mantle. Rev Geophys, 2005, 43: RG1001
10 Gutenberg B. On the layer of relatively low wave velocity at a depth of about 80 kilometers. Bull Seismol Soc Am, 1948, 38: 121–148
11 Gutenberg B. Physics of the Earth's Interior. New York: Academic Press, 1959. 240
12 Lehmann I. Velocities of longitudinal waves in the upper part of the Earth's mantle. Ann Geophys, 1959, 15: 93–118
13 Lehmann I. S and the structure of the upper mantle. Geophys J Int, 1961, 4: 124–138
14 Lehmann I. On the velocity of P in the upper mantle. Bull Seismol Soc Am, 1964, 54: 1097–1103
15 Dziewonski A M, Anderson D L. Preliminary reference Earth model. Phys Earth Planet Inter, 1981, 25: 297–356
16 Eaton D W, Darbyshire F, Evans R L, et al. The elusive lithosphere-asthenosphere boundary (LAB) beneath cratons. Lithos, 2009, 109: 1–22
17 Selway K, Ford H, Kelemen P. The seismic mid-lithosphere discontinuity. Earth Planet Sci Lett, 2015, 414: 45–57
18 Fischer K M, Ford H A, Abt D L, et al. The lithosphere-asthenosphere boundary. Annu Rev Earth Planet Sci, 2010, 38: 551–575
19 Ford H A, Long M D, Wirth E A. Mid-lithospheric discontinuities and complex anisotropic layering in the mantle lithosphere beneath the Wyoming and Superior Provinces. J Geophys Res Solid Earth, 2016, 121: 6675–6697
20 Cooper C M, Miller M S, Moresi L. The structural evolution of the deep continental lithosphere. Tectonophysics, 2017, 695: 100–121
21 Jones A G. Imaging the continental upper mantle using electromagnetic methods. Lithos, 1999, 48: 57–80
22 Artemieva I M. Global 1°×1° thermal model TC1 for the continental lithosphere: Implications for lithosphere secular evolution. Tectonophysics, 2006, 416: 245–277
23 Smythe D K, Dobinson A, McQuillin R, et al. Deep structure of the Scottish Caledonides revealed by the MOIST reflection profile. Nature, 1982, 299: 338–340
24 Brewer J A, Matthews D H, Warner M R, et al. BIRPS deep seismic reflection studies of the British Caledonides. Nature, 1983, 305: 206–210
25 McGeary S, Warner M R. Seismic profiling the continental lithosphere. Nature, 1985, 317: 795–797
26 Thybo H, Perchuć E. The seismic 8 discontinuity and partial melting in continental mantle. Science, 1997, 275: 1626–1629
27 Cook F A, van der Velden A J, Hall K W. Frozen subduction in Canada's Northwest Territories: Lithoprobe deep lithospheric reflection profiling of the western Canadian Shield. Tectonics, 1999, 18: 1–24
28 Yang W. Flat mantle reflectors in eastern China: Possible evidence of lithospheric thinning. Tectonophysics, 2003, 369: 219–230
29 Gao R, Chen C, Wang H, et al. SINOPROBE deep reflection profile reveals a Neo-Proterozoic subduction zone beneath Sichuan Basin. Earth Planet Sci Lett, 2016, 454: 86–91
30 Cook F A, Vasudevan K. Are there relict crustal fragments beneath the Moho? Tectonics, 2003, 22: 1026
31 Mareschal M, Kellett R L, Kurtz R D, et al. Archaean cratonic roots, mantle shear zones and deep electrical anisotropy. Nature, 1995, 375: 134–137
32 Vauchez A, Tommasi A, Mainprice D. Faults (shear zones) in the Earth's mantle. Tectonophysics, 2012, 558-559: 1–27
33 Calò M, Bodin T, Romanowicz B. Layered structure in the upper mantle across North America from joint inversion of long and short period seismic data. Earth Planet Sci Lett, 2016, 449: 164–175
34 Rader E, Emry E, Schmerr N, et al. Characterization and petrological constraints of the midlithospheric discontinuity. Geochem Geophys Geosyst, 2015, 16: 3484–3504
35 Tharimena S, Rychert C, Harmon N. A unified continental thickness from seismology and diamonds suggests a melt-defined plate. Science, 2017, 357: 580–583
36 Jones A G, Plomerova J, Korja T, et al. Europe from the bottom up: A statistical examination of the central and northern European lithosphere–asthenosphere boundary from comparing seismological and electromagnetic observations. Lithos, 2010, 120: 14–29
37 Gaherty J B, Kato M, Jordan T H. Seismological structure of the upper mantle: A regional comparison of seismic layering. Phys Earth Planet Inter, 1999, 110: 21–41
38 Rychert C A, Fischer K M, Rondenay S. A sharp lithosphere-asthenosphere boundary imaged beneath eastern North America. Nature, 2005, 436: 542–545
39 Thybo H. The heterogeneous upper mantle low velocity zone. Tectonophysics, 2006, 416: 53–79
40 Savage B, Silver P G. Evidence for a compositional boundary within the lithospheric mantle beneath the Kalahari craton from S receiver functions. Earth Planet Sci Lett, 2008, 272: 600–609

41 Rychert C A, Shearer P M. A global view of the lithosphere-asthenosphere boundary. Science, 2009, 324: 495–498
42 Abt D L, Fischer K M, French S W, et al. North American lithospheric discontinuity structure imaged by Ps and Sp receiver functions. J Geophys Res Solid Earth, 2010, 115: B09301
43 Yuan H, Romanowicz B. Lithospheric layering in the North American craton. Nature, 2010, 466: 1063–1068
44 Adams A, Nyblade A, Weeraratne D. Upper mantle shear wave velocity structure beneath the East African plateau: Evidence for a deep, plateauwide low velocity anomaly. Geophys J Int, 2012, 189: 123–142
45 Fishwick S, Rawlinson N. 3-D structure of the Australian lithosphere from evolving seismic datasets. Austral J Earth Sci, 2012, 59: 809–826
46 Heeszel D S, Wiens D A, Nyblade A A, et al. Rayleigh wave constraints on the structure and tectonic history of the Gamburtsev Subglacial Mountains, East Antarctica. J Geophys Res Solid Earth, 2013, 118: 2138–2153
47 Jiang M, Ai Y, Chen L, et al. Local modification of the lithosphere beneath the central and western North China Craton: 3-D constraints from Rayleigh wave tomography. Gondwana Res, 2013, 24: 849–864
48 Chen L, Jiang M, Yang J, et al. Presence of an intralithospheric discontinuity in the central and western North China Craton: Implications for destruction of the craton. Geology, 2014, 42: 223–226
49 Wirth E A, Long M D. A contrast in anisotropy across mid-lithospheric discontinuities beneath the central United States—A relic of craton formation. Geology, 2014, 42: 851–854
50 Tharimena S, Rychert C A, Harmon N, et al. Imaging Pacific lithosphere seismic discontinuities—Insights from SS precursor modeling. J Geophys Res Solid Earth, 2017, 122: 2131–2152
51 Yuan H Y, Romanowicz B. Introduction-lithospheric discontinuities. In: Yuan H Y, Romanowicz B, eds. Lithospheric Discontinuities, Geophysical Monograph Series. Washington DC: American Geophysical Union and John Wiley & Sons, Inc, 2019. 1−5
52 Kawakatsu H, Kumar P, Takei Y, et al. Seismic evidence for sharp lithosphere-asthenosphere boundaries of oceanic plates. Science, 2009, 324: 499–502
53 Hopper E, Fischer K M. The changing face of the lithosphere-asthenosphere boundary: Imaging continental scale patterns in upper mantle structure across the contiguous U.S. with Sp converted waves. Geochem Geophys Geosyst, 2018, 19: 2593–2614
54 Sun W, Fu L Y, Saygin E, et al. Insights into layering in the cratonic lithosphere beneath western Australia. J Geophys Res Solid Earth, 2018, https://doi.org/10.1002/2017JB014904
55 Kind R, Hardy M R, Yuan X H, et al. Detection of a new sub-lithospheric discontinuity in Central Europe with S-receiver functions. Tectonophysics, 2017, 700-701: 19–31
56 Yuan H, Romanowicz B, Fischer K M, et al. 3-D shear wave radially and azimuthally anisotropic velocity model of the North American upper mantle. Geophys J Int, 2011, 184: 1237–1260
57 Pavlenkova N I. General features of the uppermost mantle stratification from long-range seismic profiles. Tectonophysics, 1996, 264: 261–278
58 Teng J W, Li S L, Zhang Y Q, et al. Fine velocity structures and deep processes in crust and mantle of the Qinling orogenic belt and the adjacent North China Craton and Yangtze Craton (in Chinese). Chin J Geophys, 2014, 57: 3154−3175 [滕吉文, 李松岭, 张永谦, 等. 秦岭造山带与邻域华北克拉通和扬子克拉通的壳、幔精细速度结构与深层过程. 地球物理学报, 2014, 57: 3154−3175]
59 Sodoudi F, Yuan X, Kind R, et al. Seismic evidence for stratification in composition and anisotropic fabric within the thick lithosphere of Kalahari Craton. Geochem Geophys Geosyst, 2013, 14: 5393–5412
60 Foster K, Dueker K, Schmandt B, et al. A sharp cratonic lithosphere-asthenosphere boundary beneath the American Midwest and its relation to mantle flow. Earth Planet Sci Lett, 2014, 402: 82–89
61 Hales A L. A seismic discontinuity in the lithosphere. Earth Planet Sci Lett, 1969, 7: 44–46
62 Musacchio G, White D J, Asudeh I, et al. Lithospheric structure and composition of the Archean western Superior Province from seismic refraction/wide-angle reflection and gravity modeling. J Geophys Res, 2004, 109: B03304
63 Fuchs K, Tittgemeyer M, Ryberg T, et al. Global significance of a sub-Moho boundary layer (SMBL) deduced from high-resolution seismic observations. Int Geol Rev, 2002, 44: 671–685
64 Selway K. Electrical discontinuities in the continental lithosphere imaged with magnetotellurics. In: Yuan H Y, Romanowicz B, eds. Lithospheric Discontinuities. Geophysical Monograph Series. Washington DC: American Geophysical Union and John Wiley & Sons, Inc., 2019. 89−109
65 Leech M L. Arrested orogenic development: Eclogitization, delamination, and tectonic collapse. Earth Planet Sci Lett, 2001, 185: 149–159
66 Hopper E, Fischer K M. The meaning of midlithospheric discontinuities: A case study in the northern U.S. craton. Geochem Geophys Geosyst, 2015, 16: 4057–4083
67 Dasgupta R, Hirschmann M M. Melting in the Earth's deep upper mantle caused by carbon dioxide. Nature, 2006, 440: 659–662
68 Dasgupta R, Hirschmann M M. The deep carbon cycle and melting in Earth's interior. Earth Planet Sci Lett, 2010, 298: 1−13
69 Shankland T J, O'Connell R J, Waff H S. Geophysical constraints on partial melt in the upper mantle. Rev Geophys, 1981, 19: 394–406
70 Constable S. SEO3: A new model of olivine electrical conductivity. Geophys J Int, 2006, 166: 435–437
71 Naif S, Key K, Constable S, et al. Melt-rich channel observed at the lithosphere-asthenosphere boundary. Nature, 2013, 495: 356–359
72 Hirschmann M M. Partial melt in the oceanic low velocity zone. Phys Earth Planet Inter, 2010, 179: 60–71

73 Gaillard F, Malki M, Iacono-Marziano G, et al. Carbonatite melts and electrical conductivity in the asthenosphere. Science, 2008, 322: 1363–1365

74 Sifré D, Gardes E, Massuyeau M, et al. Electrical conductivity during incipient melting in the oceanic low-velocity zone. Nature, 2014, 509: 81–85

75 Holtzman B K. Questions on the existence, persistence, and mechanical effects of a very small melt fraction in the asthenosphere. Geochem Geophys Geosyst, 2016, 17: 470–484

76 Karato S I, Olugboji T, Park J. Mechanisms and geologic significance of the mid-lithosphere discontinuity in the continents. Nat Geosci, 2015, 8: 509–514

77 Hacker B R, Abers G A, Peacock S M. Subduction factory 1. Theoretical mineralogy, densities, seismic wave speeds, and H_2O contents. J Geophys Res, 2003, 108: 2029

78 Aulbach S, Massuyeau M, Gaillard F. Origins of cratonic mantle discontinuities: A view from petrology, geochemistry and thermodynamic models. Lithos, 2017, 268-271: 364–382

79 Eeken T, Goes S, Pedersen H A, et al. Seismic evidence for depth-dependent metasomatism in cratons. Earth Planet Sci Lett, 2018, 491: 148–159

80 Zheng J P. Mesozoic-Cenozoic Mantle Replacement and Lithospheric Thinning Beneath the Eastern China (in Chinese). Wuhan: China University of Geoscience Press, 1999 [郑建平. 中国东部地幔置换作用与中新生代岩石圈减薄. 武汉: 中国地质大学出版社, 1999]

81 Saha S, Dasgupta R, Tsuno K. High pressure phase relations of a depleted peridotite fluxed by CO_2-H_2O-bearing siliceous melts and the origin of mid-lithospheric discontinuity. Geochem Geophys Geosyst, 2018, 19: 595–620

82 Yang X. Orientation-related electrical conductivity of hydrous olivine, clinopyroxene and plagioclase and implications for the structure of the lower continental crust and uppermost mantle. Earth Planet Sci Lett, 2012, 317-318: 241–250

83 Li Y, Yang X, Yu J H, et al. Unusually high electrical conductivity of phlogopite: The possible role of fluorine and geophysical implications. Contrib Mineral Petrol, 2016, 171: 37

84 Yang X, Heidelbach F. Grain size effect on the electrical conductivity of clinopyroxene. Contrib Mineral Petrol, 2012, 163: 939–947

85 Yang X, McCammon C. Fe^{3+}-rich augite and high electrical conductivity in the deep lithosphere. Geology, 2012, 40: 131–134

86 Li Y, Jiang H, Yang X. Fluorine follows water: Effect on electrical conductivity of silicate minerals by experimental constraints from phlogopite. Geochim Cosmochim Acta, 2017, 217: 16–27

87 Chen L. Layering of subcontinental lithospheric mantle. Sci Bull, 2017, 62: 1030–1034

88 Kovács I, Lenkey L, Green D H, et al. The role of pargasitic amphibole in the formation of major geophysical discontinuities in the shallow upper mantle. Acta Geod Geophys, 2017, 52: 183–204

89 Wu S, Huang R, Xu Y, et al. Seismological evidence for a remnant oceanic slab in the western Junggar, Northwest China. J Geophys Res Solid Earth, 2018, 123: 4157–4170

90 Xu Y, Yang B, Zhang S, et al. Magnetotelluric imaging of a fossil paleozoic intraoceanic subduction zone in western Junggar, NW China. J Geophys Res Solid Earth, 2016, 121: 4103–4117

91 Granot R. Palaeozoic oceanic crust preserved beneath the eastern Mediterranean. Nat Geosci, 2016, 9: 701–705

92 Zhang J, Xiao W, Luo J, et al. Collision of the Tacheng block with the Mayile-Barleik-Tangbale accretionary complex in Western Junggar, NW China: Implication for Early-Middle Paleozoic architecture of the western Altaids. J Asian Earth Sci, 2018, 159: 259–278

93 Wang Z, Kusky T M, Capitanio F A. Ancient continental lithosphere dislocated beneath ocean basins along the mid-lithosphere discontinuity: A hypothesis. Geophys Res Lett, 2017, 44: 9253–9260

94 Wang Z, Kusky T M. The importance of a weak mid-lithospheric layer on the evolution of the cratonic lithosphere. Earth-Sci Rev, 2019, 190: 557–569

95 Fei H, Koizumi S, Sakamoto N, et al. New constraints on upper mantle creep mechanism inferred from silicon grain-boundary diffusion rates. Earth Planet Sci Lett, 2016, 433: 350–359

96 Mantisi B, Sator N, Guillot B. Structure and transport at grain boundaries in polycrystalline olivine: An atomic-scale perspective. Geochim Cosmochim Acta, 2017, 219: 160–176

97 Cawood P A, Hawkesworth C J, Dhuime B. The continental record and the generation of continental crust. Geol Soc Am Bull, 2013, 125: 14–32

98 Xu Z Q, Wang Q, Sun W D, et al. The spherical structure of the Earth and across-sphere tectonics (in Chinese). Geol Rev, 2018, 64: 261−282 [许志琴, 王琴, 孙卫东, 等. 地球的层圈结构与穿越层圈构造. 地质论评, 2018, 64: 261−282]

99 Ren J S, Xu Q Q, Zhao L, et al. Looking for submerged landmasse (in Chinese). Geol Rev, 2015, 61: 969−989 [任纪舜, 徐芹芹, 赵磊, 等. 寻找消失的大陆. 地质论评, 2015, 61: 969−989]

100 Lustrino M, Anderson D L. The mantle isotopic printer: Basic mantle plume geochemistry for seismologists and geodynamicists. In: Foulger G R, Lustrino M, King S D, eds. The Interdisciplinary Earth: A volume in Honor of Don L. Anderson. Washington DC: Geological Society of America Special Paper 514 and American Geophysical Union Special Publication, 2015, 71: 257–279

101 Cammarano F, Romanowicz B. Insights into the nature of the transition zone from physically constrained inversion of long-period seismic data. Proc Natl Acad Sci USA, 2007, 104: 9139–9144

102 French S, Lekic V, Romanowicz B. Waveform tomography reveals channeled flow at the base of the oceanic asthenosphere. Science, 2013, 342: 227–230

Summary for “岩石圈中部不连续面的成因及其动力学意义”

The origins and geodynamic implications of mid-lithospheric discontinuities

Yixian Xu[1*], Jianping Zheng[2], Xiaozhi Yang[3] & Qunke Xia[1]

[1] *School of Earth Sciences, Zhejiang University, Hangzhou 310027, China;*
[2] *School of Earth Sciences, China University of Geosciences, Wuhan 430074, China;*
[3] *School of Earth Sciences and Engineering, Nanjing University, Nanjing 210023, China*
* Corresponding author, E-mail: xyxian@zju.edu.cn

Geophysical, petrological and geochemical studies have shown that the lithospheric mantle is highly heterogeneous in its physical properties and chemical compositions. They provide critical information on the evolution of the lithosphere-asthenosphere boundary (LAB). Considerable efforts by geophysical approaches have demonstrated that LAB is characterized by profound changes in physical properties such as seismic velocities and electrical resistivity at an average depth of ~70 km in the oceanic areas. In the continental regions, however, the variations in the physical properties at LABs are not that significant and their depths vary greatly with tectonic environments (e.g., orogens vs. cratons). Mid-lithospheric discontinuities (MLDs; ~60 to 120 km depths) have been equally well documented by various techniques, including deep seismic reflections and refractions, receiver functions analyses of teleseismic Ps and Sp phases, teleseismic and ambient-noise based surface-waves tomography. Except in some regional cases, MLDs are usually featured by reduced velocities (i.e., negative velocity gradients). It appears that MLDs are statistically correlated with the low-resistivity layers, as imaged for the European continent.

Many hypotheses have been proposed to explain the origin of MLDs, including the accumulation of volatile-bearing assemblages due to metasomatism of magmas/fluids and/or metamorphism; the change of deformation patterns of rocks in the lithospheric mantle and finally a “frozen” LAB. Here we review the related advances and try to reconcile available data and models. We first provide a brief introduction about the discovery of MLDs, by summarizing their velocity, radial and azimuthal anisotropies as well as their internal structures across Australian, North American and Euro-Asian continents. Then we discuss the possible origin of MLDs, by considering mantle heterogeneities in mineralogy and petrology and in particular the potential role of volatile-rich minerals such as phlogopite, amphibole and carbonates. Finally, we conclude that MLDs may be frozen LABs. It sheds light on the potential importance of MLDs in Earth’s evolution and especially the global tectonic and the changes over time.

We present a working hypothesis using a dynamically-evolved LAB model. MLDs began as oceanic LABs, with their depths increasing gradually from the mid-ocean ridges to subduction zones due to change in temperature and age. During continental accretion, the “inherited” oceanic LAB merged with the continental lithosphere and became deepened along with the cooling of the new continental lithosphere. In brief, the old LAB was “frozen” into the continental lithosphere and produced MLDs. Several possible mechanisms supporting this hypothesis are proposed, and the conditions that are tenable from recent results of geodynamic modeling studies in Africa are presented. The advantages of this hypothesis are highlighted. Its potential in explanation of scientific puzzles of solid earth is evaluated.

mid-lithospheric discontinuities (MLDs), negative velocity gradients (NVGs), high electrical conductivity layer (HCL), anisotropy, hydrous minerals, plate tectonics

doi: 10.1360/N972019-00161